2-19-2019

# Forcespinning technique for the production of poly(d,l-lactic acid) submicrometer fibers: Process–morphology–properties relationship

Victoria Padilla-Gainza

Graciela Morales

Heriberto Rodríguez-Tobías

Karen Lozano

Morales Graciela (Orcid ID: 0000-0003-0714-4325)
Rodríguez-Tobías Heriberto (Orcid ID: 0000-0003-1573-1829)

# Forcespinning technique for the production of poly(D,L-lactic acid) sub-micron fibers: Process-Morphology-Properties Relationship

Victoria Padilla-Gainza[1], Graciela Morales[1], Heriberto Rodríguez-Tobías[1], Karen Lozano[2]

[1] Centro de Investigación en Química Aplicada, Boulevard Enrique Reyna Hermosillo N° 140. C.P. 25294. Saltillo, Coahuila, Mexico

[2] Mechanical Engineering Department, University of Texas Rio Grande Valley, 1201 W. University Dr. Edinburg TX, 78539

Corresponding author(s): Graciela Morales (E-mail: graciela.morales@ciqa.edu.mx),

Heriberto Rodríguez-Tobías (E-mail: lcq.heriberto.rodriguez@gmail.com)

## ABSTRACT

This work addresses a systematic study for the process development and optimization of poly(D,L-lactic acid) PDLLA sub-micron fibers utilizing the centrifugal spinning technique known as Forcespinning®. This study analyzes the effect of polymer concentration (8, 10, and 12 wt.%) and angular speed on the fiber morphology, diameter distribution, and fiber yield. The increase in polymer concentration and angular speed favored the formation of continuous and homogeneous sub-micron fibers with an absence of bead formation and higher output. The optimal conditions were established considering the morphological characteristics that exhibit a greater surface area (homogeneous and sub-micron fibers); and they were achieved at a polymer concentration of 10 wt.% at an angular speed ranging from 8000 rpm to 10000 rpm. Optimization of PDLLA sub-micron fiber fabrication lays the groundwork for scaling up the process and serves as a platform to further develop promising applications of PDLLA nonwoven mats, particularly in the biomedical area such as in scaffolds for tissue engineering.

## 1. INTRODUCTION

In recent years the production of sub-micron fibers in the biomedical area has garnered considerable relevance given its attractive characteristics such as high surface area, high porosity, and ability to tailor pore size. These systems resemble the extracellular matrix, and therefore have great potential to be used in tissue regeneration[1,2]. Several methods have been explored to fabricate these sub-micron fibers, such as: melt blowing,[3] phase separation,[4] template synthesis,[5] and electrospinning.[6] Although,

electrospinning is highly popular, there are several disadvantages that have prevented its industrial production and therefore ultimate use for practical applications. This system produces minute amounts of fibers (~0.1 g/h), requires highly toxic organic solvents with specific dielectric properties, and presents a high cost of operation due to the need of high electric fields.[7] Forcespinning® (FS), was recently introduced with the potential of alleviating the aforementioned disadvantages found within the electrospinning technique. FS utilizes centrifugal forces instead of electric fields, and fibers can be produced either from a polymeric solution or molten polymer. When a polymeric solution is used for producing fibers, the solvent employed does not require specific dielectric properties since there is an absence of an electric field, therefore it broadens the materials that can be used to produce fine fibers. Its yield has been reported as 50-100 gr/h at lab scales and hundreds of meters per minute at industrial scale.[8–10] Figure 1 shows a basic scheme of the FS process. The process starts by placing the solution or pellets in the spinneret (Figure 1(A) depicts a spinneret for solution-based systems and used at a lab scale apparatus, spinnerets used at industrial scale systems do not use needles). As the angular speed is increased, it reaches a critical value where the centrifugal force exceeds the surface tension of the polymeric solution or melt, and fine fibers emerge from the tip of the needles following the developed aerodynamic field until they are deposited in the outer collector. Figure 1(B) depicts the direction and therefore friction with the air, which results in fiber stretching and thinning while solvent evaporates or melt cools down.

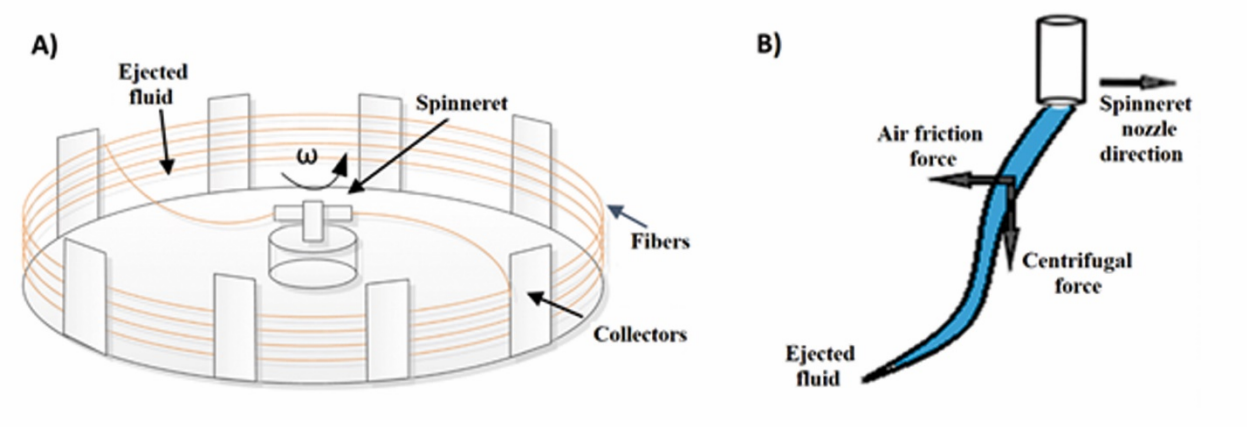


**Figure 1**. (A) Basic configuration for the FS system and (B) fiber formation as the solution leaves the spinneret.

Different morphologies can be obtained when spinning a polymer solution; beads, fibers with beads, and fibers without beads (homogeneous systems). The fiber morphology is strongly related to instability principles such as the Rayleigh-Plateu.[11–13] The rheological properties of the system coupled with the selected spinning parameters will dictate the influence of various instabilities. In this sense when the solution does not possess a critical polymeric chain entanglement, a spraying process will be favored thus forming polymer beads or beads-on-strings. On the other extreme, if the entanglement is too high, the applied centrifugal force might not be enough to overcome the surface tension of the polymeric fluid and will prevent the generation of fibers.[12] The fiber morphology, namely diameter and porosity, strongly depends on viscosity and surface tension; which in turn intrinsically depend on molecular weight and polydispersity of the selected polymer, while extrinsically, the dependence is on the polymer concentration within the solution, selected solvent, and additives used to prepare the solution. It has been demonstrated that different process parameters would affect fiber formation. In this context, the spinneret configuration influences the fiber elongation/orientation, the angular speed greatly affects the forces that produce the fiber elongation, [9,11,12,14] the spinneret nozzle-to-collector distance directly influences the flight time of the ejected fluid which has an impact on solvent evaporation,[6] and the environmental conditions (temperature and humidity) affect solvent evaporation rate and fiber surface morphology.[15,16]

In this regard, several reports have been published. For example, Padron *et al.*[9] studied the effect of spinneret filling, geometry and orientation of the needle, angular speed, and polymer concentration on the ultimate fiber diameter of polyethylene oxide fibers. They concluded that in the FS method, the angular speed and polymer concentration were the most significant variables for fiber production. For a 6 wt.% PEO solution, average fiber diameters of 315 nm and 130 nm were obtained for an angular speed of 2500 and 6000 rpm, respectively. Increasing polymer concentration to 10 wt.% increased the fiber diameter from 130 to 400 nm for samples spun at 6000 rpm.

Badrossamay *et al.*[11] studied the influence of the nozzle geometry at different angular speeds (4000, 8000, and 12000 rpm) for poly(L-lactic acid) (PLLA) at concentrations of 4, 6, 8, and 10 wt.%, using centrifugal spinning. The authors reported that low polymeric concentrations produced mostly beads; meanwhile homogeneous fibers were mainly obtained at 8 wt.%, independently of the selected angular speed. Further increasing concentration up to 10 wt.% produced homogeneous fibers only at 12000 rpm. These behaviors were explained in terms of the degree of entanglement and stability of the polymeric fluid.

Ren *et al.*[12] worked with mixtures of PLLA and polyvinylpyrrolidone (PVP), and reported the influence of polymer concentration (5, 8 y 10 wt.%) and angular speed (3500, 5000, 7000 and 9000 rpm) on the morphology and average fiber diameter of the fibers engineered by FS. Homogeneous fibers composed entirely of PLLA, were obtained at a polymer concentration of 8 and 10 wt.% at all evaluated speeds, except for 3500 rpm. In the case of the polymer blends, it was observed that by increasing the concentration of PLLA in the blend, fiber production was facilitated. Following a similar premise, Lu *et al*.[14] reported a decrease in fiber diameter at low concentrations of polyacrylonitrile when exposed to high angular speed. Conversely, Vasquez *et al.*[17] studied the effect of angular speed and concentration of poly(vinyl difluoride) on fiber morphology obtained by FS, and reported that the diameter was not significantly altered when changing angular speed from 4000 to 8000 rpm, for polymer concentrations of 18 and 21.5 wt.%, respectively. Recently, Serthat *et al.* [18] reported an optimization study for the production of sub-micron fibers of thermoplastic polyurethane (TPU), and identified (among three studied variables: nozzle diameter, angular speed, and polymer concentration) that the polymer concentration has the greatest effect on fiber diameter, with a contribution of 77.5%.

The production of homogeneous fibers is not a trivial issue as demonstrated by the previously cited publications, and in the case of PDLLA there is a lack of background related to centrifugally spun fibers. For this reason, this article reports a systematic study to determine the optimum processing parameters for obtaining sub-micron PDLLA fibers by means of the FS technique. The opportunity to find optimum parameters for the production of PDLLA nonwoven systems will open up the door to further research on the potential use of these nonwoven fiber mats as materials for tissue engineering.

## 2. EXPERIMENTAL SECTION

### *2.1 Materials*

Poly(D,L-lactic acid) (PDLLA) was purchased from NatureWorks LLC (Ingeo 6362D) with an average molecular weight of 160 kg·mol$^{-1}$ and a polydispersity of 1.65. Chloroform was purchased from Fisher Scientific and used as received.

### *2.2 Preparation of the PDLLA precursory solutions*

In the study reported herein, polymeric solutions were employed to obtain the fibrous materials and they were prepared by dissolving the corresponding amount of PDLLA pellets in chloroform[11] in order to

obtain polymer concentrations of 8, 10, and 12 wt.%. The solutions were magnetically stirred for 22 hours at room temperature in properly closed glass vials. Before processing the solutions by the Forcespinning® technique, rheological studies of the resulting precursory solutions were performed in an Anton Paar rheometer (MCR 301) with a cone-plate system (50 mm in diameter, angle of 2° and a gap of 0.205) at 25°C.[19]

### *2.3 Forcespinning® of the PDLLA-based solutions*

The developed solutions were subjected to centrifugal spinning using a Cyclone L-1000M from Fiberio Technology Corporation. A cylindrical spinneret equipped with two 30-gauge needles (0.5 inches in length), and an eight-pillar collector system positioned 15 cm away from the tip of the needles were used. In each run, the spinneret was filled with 2 mL of polymeric solution, and the Forcespinning® process was conducted at room temperature (23-25°C and at a relative humidity of 59 ± 9%)[9]. Two sets of materials were engineered, for the optimization, only one Forcespinning® run was carried out, while for the mats fabricated under optimal conditions, 7 runs were needed. After collection of the centrifuged samples, the samples were placed in an oven at 30°C under vacuum for 24 hours to remove solvent residues[20]. Finally, the obtained mats were stored in plastic bags with desiccant to prevent moisture absorption.

As previously described by several authors[9,11,12,14], polymer concentration and angular speed have been deemed as the parameters that effectively influence the process. Table 1 shows the variables used in this study. Fiber yield ($\eta_p$) (equation 1) and feasibility of fiber collection (fiber deposition that allows the collection of homogenous nonwoven fiber mats) were among other studied parameters.

Equation 1 estimates the production of fibrous material that can be obtained under the operating conditions of the Forcespinning® ($\boldsymbol{\eta}_P$). For the calculation, the total solids (quantity of polymer) contained in 2 mL (the volume used in each run) of the polymeric solution were taken as the reference; assuming a yield of 100% of transformation of the total solids into fibrous material.

$$\eta_P = \frac{W_f}{TS} x100 \qquad (1)$$

where, $W_f$ and *TS* are the weight of the collected fiber per run (5 min) and total solids contained in 2 mL of solution, respectively.

**Table 1**. Parameters analyzed during the optimization process in the production of centrifugally PDLLA spun fibers

| Variables | Levels | | |
|---|---|---|---|
| Concentration of PDLLA (wt.%) | 8 | 10 | 12 |
| Angular Speed $\times 10^{-3}$ (rpm) | 4-10 | 4-10 | 4-10 |

### *2.5 Materials characterization*

Morphological analysis of the obtained materials was performed in a scanning electron microscope (Sigma VP, Carl Zeiss). The images were utilized for estimating the average fiber diameter by using the software ImageJ version 1.48, 100 fibers were measured per sample taken from at least 20 fibers per micrograph and conducting 3 measurements per fiber, thus resulting in 300 measurements.

The optimized PDLLA mats were further analyzed by means of thermogravimetric analysis (TGA) (TA Instruments, Q400) and differential scanning calorimetry (DSC) (TA Instruments, Q200). In the case of TGA, the samples were heated from 30°C to 600°C at a heating rate of 10°C/min under $N_2$ atmosphere (flow rate = 40 mL/min). In the case of DSC, the samples were subjected to a heating-cooling-heating cycle at a heating rate of 10°C/min from -70°C to 200°C. For the sake of comparison, the same thermal analyses were carried out for PDLLA pellets (raw material).

## 3. RESULTS AND DISCUSSION

This section is divided in three sub-sections. The first one (3.1) presents the rheological behavior of the developed PDLLA solutions at 8, 10 and 12 wt.%. The second one (3.2) addresses the relation between processing parameters and fiber morphology, thus establishing the optimal conditions for the fabrication of PDLLA mats. The third section (3.3) focuses on the characterization of the PDLLA mats fabricated under the optimum conditions found in 3.2 to produce fibers with < 1 µm diameters.

### *3.1 Rheological behavior of the developed solutions*

The viscosity of polymer solutions that will be subjected to the spinning process is a key property since it can be associated with chain entanglements. In this context, the viscosity of the developed solutions with different PDLLA concentration was evaluated as a function of shear rate, and the corresponding

values are plotted in Figure 2. PDLLA solutions exhibited negligible changes within the analyzed range of shear rate (1-1000 $s^{-1}$). The usual pseudo-plastic behavior of PDLLA was not observed, the fluid tended to be Newtonian, especially for the 8 and 10 wt.% samples, since the systems consisted of diluted solutions. It can be observed that the viscosity values increased proportionally with PDLLA concentration up to almost one order of magnitude, thus suggesting the formation of chain entanglements. It is important to clarify that although the rheological studies presented herein were performed in a range of shear rate lower than that applied in a centrifugal spinning equipment, changes in viscosity can be neglected given that the PDLLA solutions were Newtonian fluids.

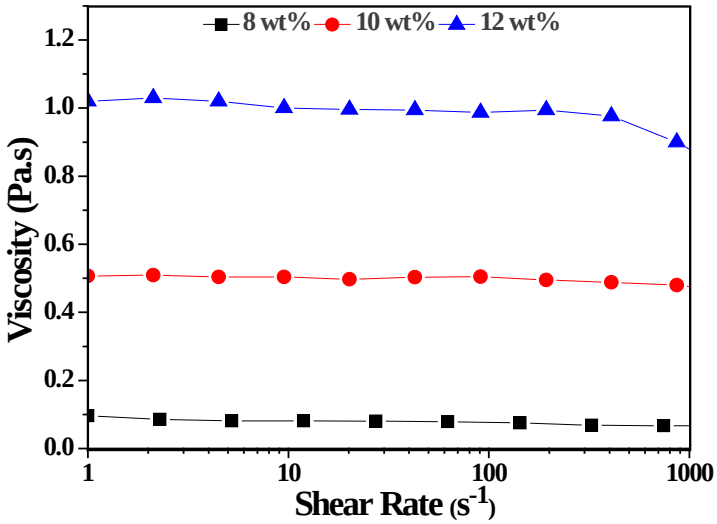


**Figure 2**. Viscosity as a function of shear rate and concentration of PDLLA solution ($CHCl_3$ was used as the solvent at 25°C).

For the level of chain entanglement of PDLLA in chloroform, the solution entanglements number $(n_e)_{sol}$, was estimated using equation 2, previously reported by Shenoy *et al.*[13]

$$(n_e)_{sol} = \frac{\emptyset_p M_w}{M_e} \qquad (2)$$

where, $\emptyset_p$ is the volumetric fraction of the polymer, $M_w$ is the weight average molecular weight, and $M_e$ is the entanglement molecular weight (average molecular weight between entanglement junctions).[21] The value of $M_e$ for the PDLLA used in this work was obtained from literature and was equal to 5600 g·mol$^{-1}$. [22] The calculated $(n_e)_{sol}$ values were 2.82, 3.53 and 4.24 for 8, 10 and 12 wt.%, respectively. Shenoy *et al.*[13] claimed that in the case of a polymer solution (polymer with a dispersity lower than 2)

subjected to electrospinning, there is a critical value of $(n_e)_{sol}$ equal to 3.5, above which fibers with homogeneous morphology can be obtained. For the case of centrifugally spun polymeric fibers, there is no evidence that the same hypothesis applies, if so, only the PDLLA solutions in a concentration higher than 10 wt.% would generate homogenous fibers, which will be addressed in a subsequent section.

### *3.2 Influence of processing parameters on the morphology of PDLLA-based materials*

In order to elucidate the effect of important parameters, namely angular speed and solution concentration on the final morphology of the centrifugally engineered PDLLA structures, these were analyzed by electron microscopy and the corresponding series of SEM micrographs are depicted in Figure 3-5. At first instance, the effect of PDLLA solution concentration on the morphology of the obtained materials could be perceived. At 8 wt. % (Figure 3), most of the materials are composed by beads and beaded fiber, while samples derived from solutions at 10 and 12 wt.% (Figures 4 and 5, respectively) resulted in a more homogeneous fibrous morphology, except for the solution of 10 wt.% spun at 4000 rpm. This finding confirms that the $(n_e)_{sol}$ values, 3.53 and 4.24 for 10 and 12 wt.% respectively (see previous section), can roughly predict the critical concentration to produce homogeneous polymeric fibers. It is important to note that fiber formation is driven by the intrinsic properties of the fluid and the forces that act upon it. At low concentrations, bead formation is expected given that as the fluid is ejected through the nozzle, it reaches a critical length and once the solvent evaporates it reverts into droplets, and later into beads. This occurs as a result of the surface tension, due to the fluid cohesion forces restrict the fluid elongation, confining it to a smaller surface (drops = beads) and it is known as the Rayleigh-Plateau instability.[23,24] As the level of entanglement increases, the jet is more stable and eventually leads to fiber formation upon solvent evaporation.

Figure 3-5 also show the influence of the angular speed on the morphology of the obtained PDLLA fibers. Ren *et al.*[12] reported the formation of PLLA fibers produced by centrifugal spinning methods at different processing conditions. Their results showed that as the angular speed is increased, the centrifugal force is consequently increased, and the resultant force then exceeds the fluid resistance to be elongated, thus promoting the formation of homogeneous fibers. In this work, equivalent results were found at a PLLA concentration of 8 wt.%, where a significant reduction of beads was observed as the angular speed was increased. For the 10 wt.% samples, homogeneous fibers were obtained as the speed exceeded 5000 rpm, just as explained by Ren *et al*.[12]

The change in morphology was quantitatively monitored through the fiber diameters, which were plotted as box charts in Figure 6 (the box denotes the 50% of diameter population between quartile 1 ($Q_1$) and quartile 3 ($Q_3$)) and represented in Table 2. The higher concentration of PDLLA (12 wt.%) promoted the formation of thicker fibers, ranging in the interval $Q_1$-$Q_3$ from 0.5 to 1.5 µm approximately, compared to the fibers obtained using a more diluted solution (10 wt.%) whose values were mostly lower that 1 µm. This fact can be explained in terms of the rheological behavior, since higher viscosities will require longer relaxation times to fully elongate the ejected fluid.[25,26]

Furthermore, a strong influence of the angular speed on the fiber diameter was evidenced for the materials spun from 10 wt.% solution. As it can be seen in Figure 6 and Table 2, the diameters of the interval $Q_1$-$Q_3$ experimented a shift to smaller diameters from 0.436-1.276 to 0.317-0.716 µm for the samples spun at 7000 and 9000 rpm, respectively. This result indicates that the centrifugal force associated with angular speeds ≥ 8000 rpm was enough to allow the elongation of the polymeric fluid. With respect to the materials derived from the 12 wt.% solution, relatively homogeneous fibers were obtained through the whole range of speeds without a significant variation in fiber diameter as previously noted by Vasquez *et al.*[17] for PVDF fibers. The dissimilar behavior of the PDLLA solutions at 10 and 12 wt.% can be explained by higher viscous forces (higher chain entanglements) at 12 wt.% than those at 10 wt.% thus preserving the diameter of the polymeric jet and consequently the dimensions of the resulting fibers, while the lower viscous forces at 10 wt.% enables the thinning of the polymeric jet.

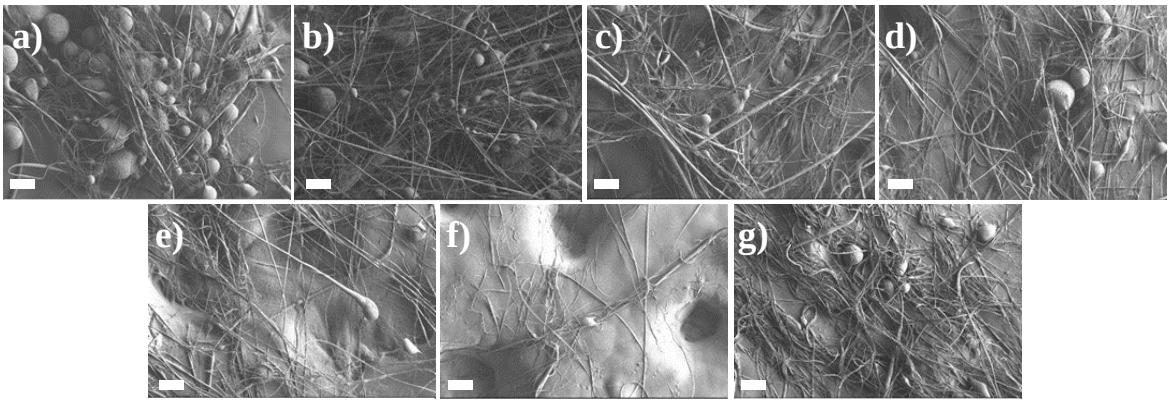


**Figure 3.** SEM micrographs of PDLLA fibers obtained from 8 wt.% solutions centrifugally spun at (a) 4000, (b) 5000, (c) 6000, (d) 7000, (e) 8000, (f) 9000 and (g) 10000 rpm (the scale bar is 20 µm).

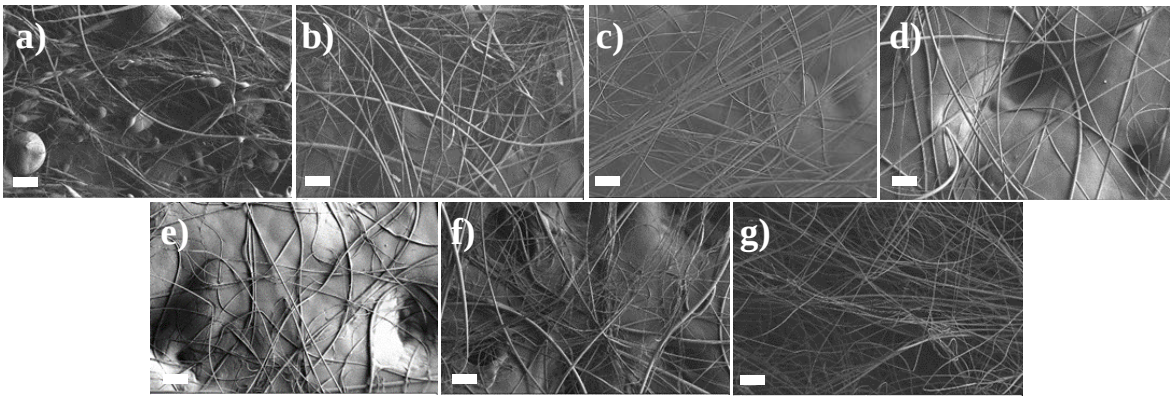


**Figure 4**. SEM micrographs of PDLLA fibers obtained from 10 wt.% solutions centrifugally spun at (a) 4000, (b) 5000, (c) 6000, (d) 7000, (e) 8000, (f) 9000 and (g) 10000 rpm (the scale bar is 20 μm).

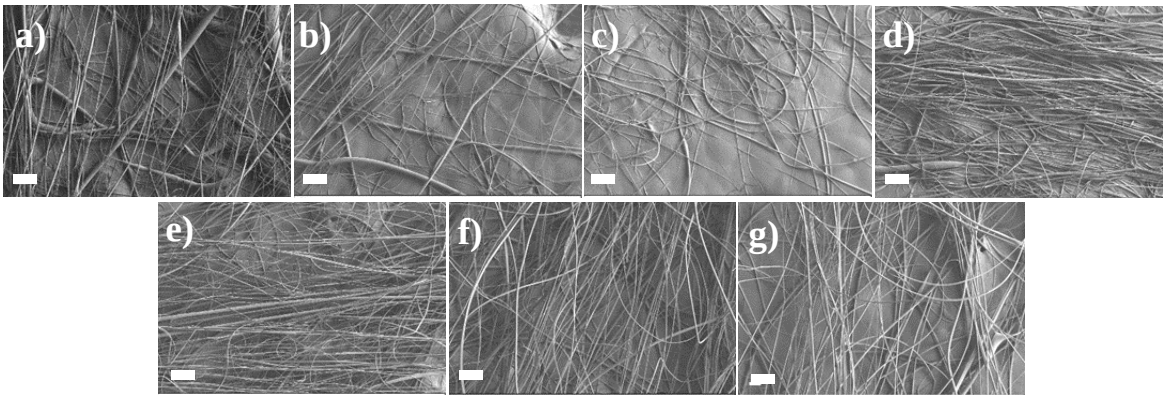


**Figure 5**. SEM micrographs of PDLLA fibers obtained from 12 wt.% solutions centrifugally spun at (a) 4000, (b) 5000, (c) 6000, (d) 7000, (e) 8000, (f) 9000 and (g) 10000 rpm (the scale bar is 20 μm).

**Table 2**. Morphological and statistical parameters of the homogeneous PDLLA fiber systems obtained by centrifugal spinning at different polymer concentrations (10 and 12 wt.%) and angular speeds (5000-10000 rpm) with their corresponding process yield ($\eta_P$).

| | 10 wt.% | | | 12 wt.% | | |
|---|---|---|---|---|---|---|
| Angular speed (rpm) | $Q_1$-$Q_3$ (μm) | $\overline{D_f}$ (μm) | $\eta_p$ (%) | $Q_1$-$Q_3$ (μm) | $\overline{D_f}$ (μm) | $\eta_p$ (%) |
| 5000 | 0.34-1.42 | 1.12±1.16 | 56.7 | 0.71-1.56 | 1.18±0.63 | 30.4 |

| | | | | | | |
|---|---|---|---|---|---|---|
| 6000 | 0.39-1.07 | 0.93±0.87 | 76.1 | 0.78-1.40 | 1.12±0.49 | 43.6 |
| 7000 | 0.44-1.28 | 1.03±0.78 | 66.3 | 0.74-1.61 | 1.18±0.62 | 54.6 |
| 8000 | 0.22-0.61 | 0.55±0.52 | 60.9 | 0.70-1.13 | 0.97±0.39 | 73.0 |
| 9000 | 0.32-0.72 | 0.57±0.38 | 61.7 | 0.67-1.19 | 0.95±0.35 | 73.7 |
| 10000 | 0.27-0.50 | 0.46±0.36 | 51.4 | 0.56-1.41 | 1.10±0.68 | 68.7 |

Q1= quartile 1, Q3= quartile 3 and $\overline{D_f}$ = average fiber diameter.

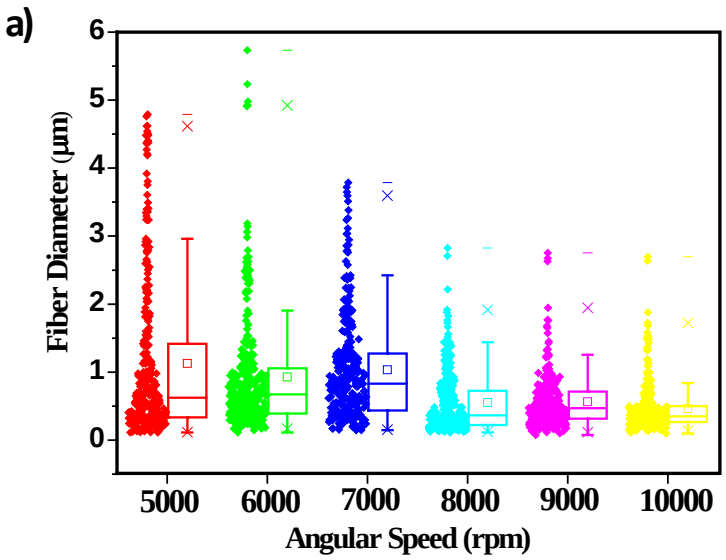

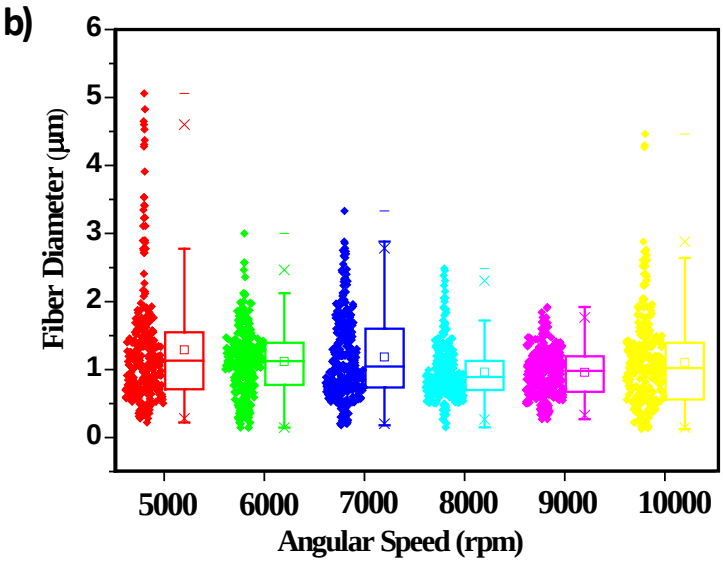


**Figure 6.** Box charts of PDLLA fiber diameter as a function of angular speed applied to solutions containing 10 (a) and 12 (b) wt.% of PDLLA in chloroform. Boxes indicate the interquartile range (IQR) between $Q_1$ and $Q_3$, the upper and lower whiskers represent 1.5 times the IQR and the minimum value of the distribution, respectively. The horizontal line is the median, the small square inside the box is the mean (the average fiber diameter, $\overline{D_f}$ ) and the points next to the box are the dispersion values.

Centrifugally spun PDLLA fibers exhibited another interesting morphological characteristic, which can be observed in the SEM micrographs shown in Figure 7. The fibers showed a rough surface along the entire structure, and this characteristic was independent of processing conditions. This surface structure is the result of using a highly volatile solvent in combination with relatively high atmospheric humidity *ca.* 60% as it has been observed by other authors in fibers obtained by either electrospinning or centrifugal spinning.[13,16,27] It is noteworthy to mention that the obtained PDLLA fibers have contrasting morphologies at the core and its surface. There is no presence of pores in the core of the fibers, as corroborated by SEM images from the cross-section of the fibers. Considering the study reported by Natarajan *et al.*[28], thermally induced phase separation (TIPS) is the mechanism that can explain the aforementioned morphological characteristics of spun PDLLA fibers. The TIPS mechanism is based on the phenomenon produced when the temperature is suddenly decreased due to flash solvent evaporation. This event leads to a thermodynamic instability of the fluid, inducing phase separation of polymer-rich and solvent-rich domains. In addition, the cooling generates water vapor condensation from the air into

droplets on the jet surface. Therefore, in the elongation and solidification process the polymer-rich domain forms the fiber matrix, whereas the solvent-rich domain and water droplets control the fiber surface granting its rough appearance, as pores or small cavities.[29,30]

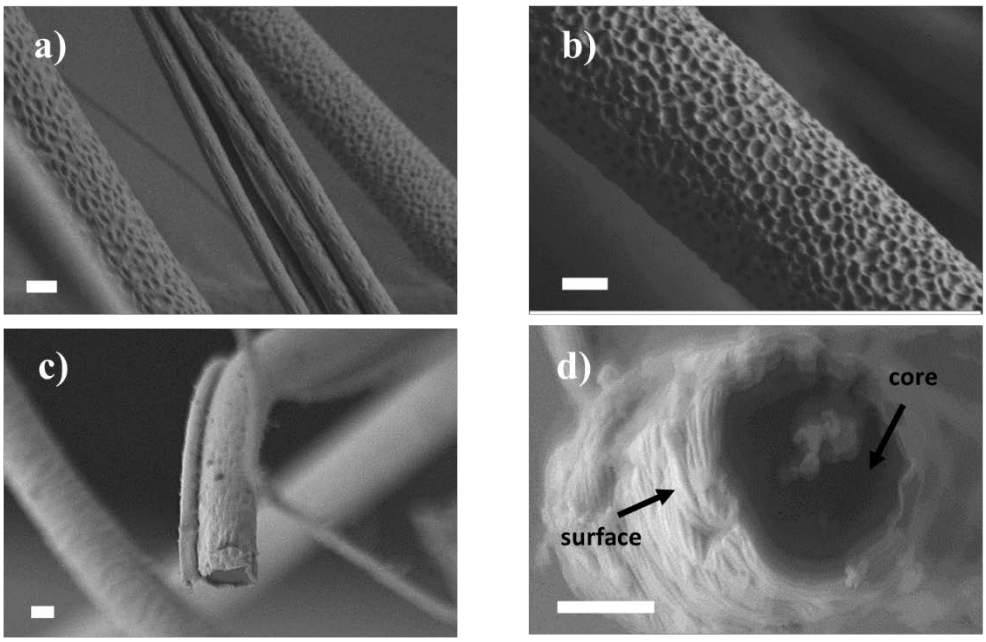


**Figure 7**. SEM micrographs of PDLLA fibers depicting a rough surface (a-b) and cross-section (c–d), which were engineered from a solution of 10 wt.% at 9000 rpm (the scale bar is 1 µm).

The obtained results provide the ideal concentration and angular speed for obtaining PDLLA fibers with homogeneous morphology and average diameter lower than 1 µm. PDLLA solutions of 10 wt.% subjected to an angular speed ≥ 8000 rpm were prone to generate sub-micron fibers. However, only those PDLLA fibers obtained at an angular speed of 9000 rpm were selected for the fabrication of mats due to fiber collection feasibility, narrow dispersion of diameter values and higher throughput (61.7%) in comparison with the system obtained at 8000 rpm (60.9%) and 10000 rpm (51.4%) (Table 2). It is important to emphasize that the mats were manufactured under the selected conditions and description established in the experimental section.

### *3.3. Morphological and thermal characterization of mats based on submicron PDLLA fibers*

The engineered PDLLA mats showed homogeneous fibrous morphology under the conditions previously selected (see Figure 8). However, the diameters of the interval $Q_1$-$Q_3$ experimented a shift to higher values compared with the fibers obtained in the optimization stage, from 0.317-0.715 to 0.355-1.075 µm. This behavior could be attributed to a slight variation on the centrifugally formed polymer jet throughout the seven runs used in this case for obtaining the corresponding mat. The porosity (Ø) of the mat was calculated using equation 3.[29]

$$\emptyset = \left(1 - \frac{m}{Z*A*H*\rho}\right)*100 \qquad (3)$$

where, *m*, *Z*, *A*, *H* and *ρ*, are the mass of the mat, thickness, width, length and density, respectively. The Ø value was higher than 90%, thus suggesting that this mat is highly promising for application related to tissue engineering.[31]

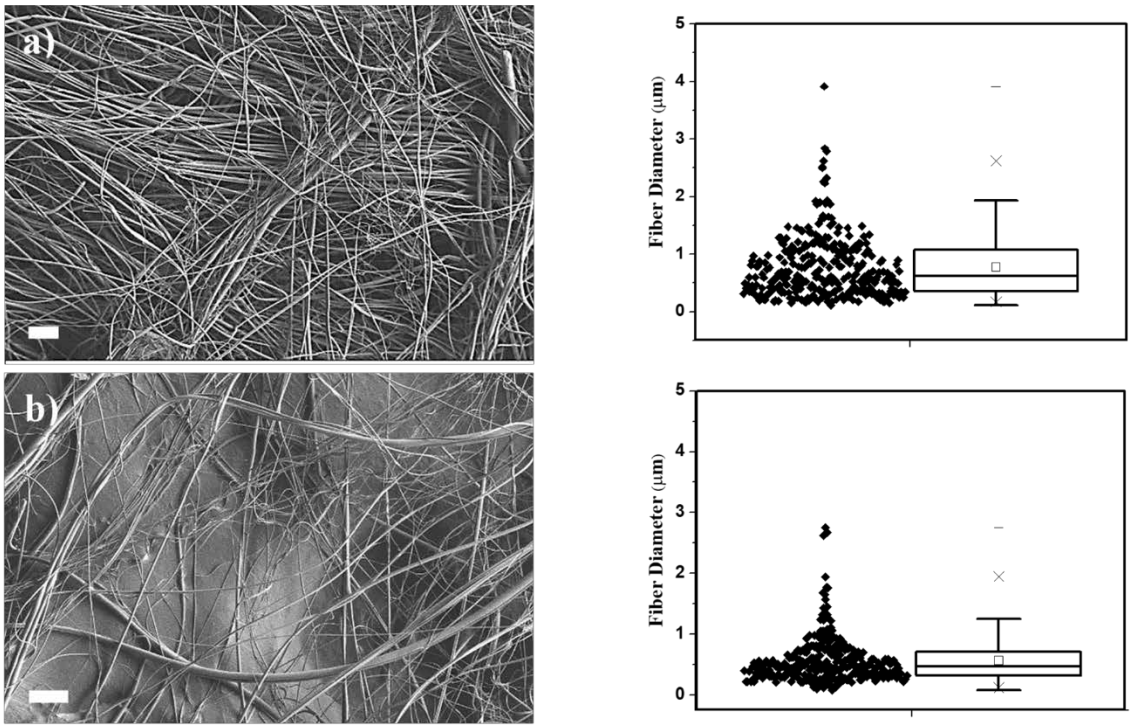


**Figure 8.** SEM images of PDLLA fibers obtained (a) in the form of a mat (7 runs) and (b) in the

optimization stage (1 run). The corresponding box charts of fiber diameters are presented on the right side (scale bar is 20 µm).

Fundamental thermal properties of PDLLA mats were assessed by TGA and DSC analysis. Figure 9a illustrates the thermal degradation pattern of centrifugally spun PDLLA mats and the corresponding bulk material (PDLLA pellets). It could be perceived that the fibers had two mass losses, the first one started at 62°C and ceased at 96°C, while the second one initiated at 284°C up to 381°C. The mass loss at the lower temperature range could be associated with the evaporation of residual solvent (boiling point of chloroform = 61°C at 760 mm Hg) and the mass loss at the higher temperature range is attributed to the degradation of PDLLA.[32] These mass losses are clearly observed in the corresponding derivative TGA shown in Figure 9b, in which two peaks are evidenced and can be assigned to the maximum weight loss. Conversely, PDLLA in the form of pellets showed only one degradation step which started at higher temperature when compared to the PDLLA fibers (ca. 289°C). This delayed degradation could be explained in terms of material surface area exposed to the heat source.[33]

Regarding the thermal transitions of the centrifugally engineered PDLLA mats, DSC thermograms are depicted in Figure 10. It could be observed an endothermic transition at 59°C occurring during the first heating. This behavior denotes the presence of an ordered phase of polymer chains, which can be attributed to the uniaxial stretching of the polymeric fluid produced by the centrifugal force during the spinning process. The same behavior was observed for the bulk material, thus suggesting that the tensile stress applied during the processing of PDLLA promoted partial alignment of the polymer chains. On the other hand, the thermograms of cooling and second heating exhibited the characteristics of an amorphous polymer, as expected. Similar results have been reported for fibers production by electrospinning,[34] melt-spinning[35] and wet spinning method.[36]

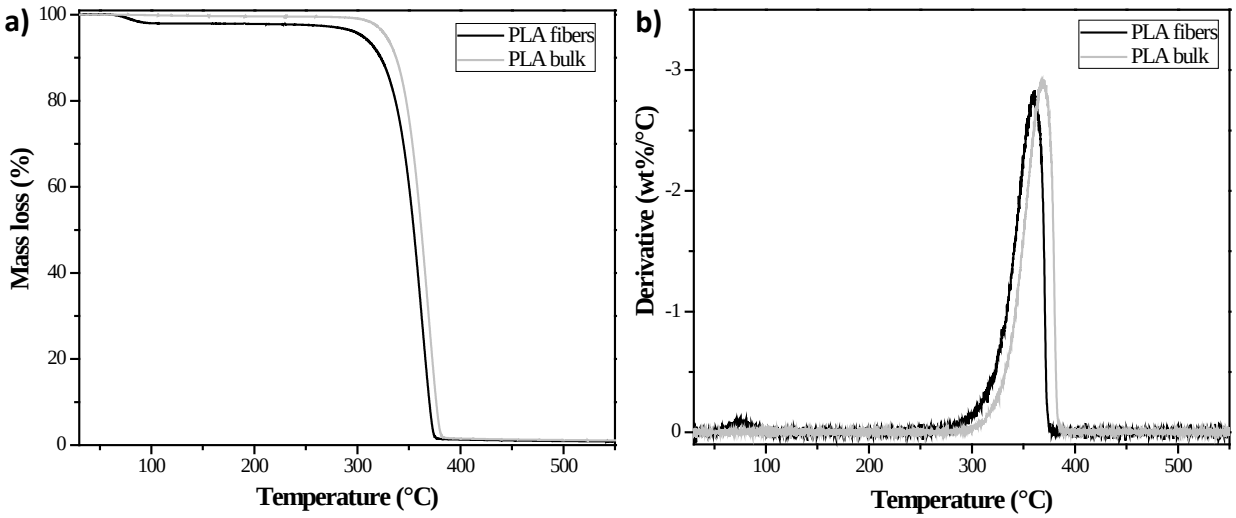


**Figure 9**. (a) Degradation patterns derived from TGA of the centrifugally spun PDLLA fibers obtained and pellets (bulk), and (b) the corresponding derivative graphs.

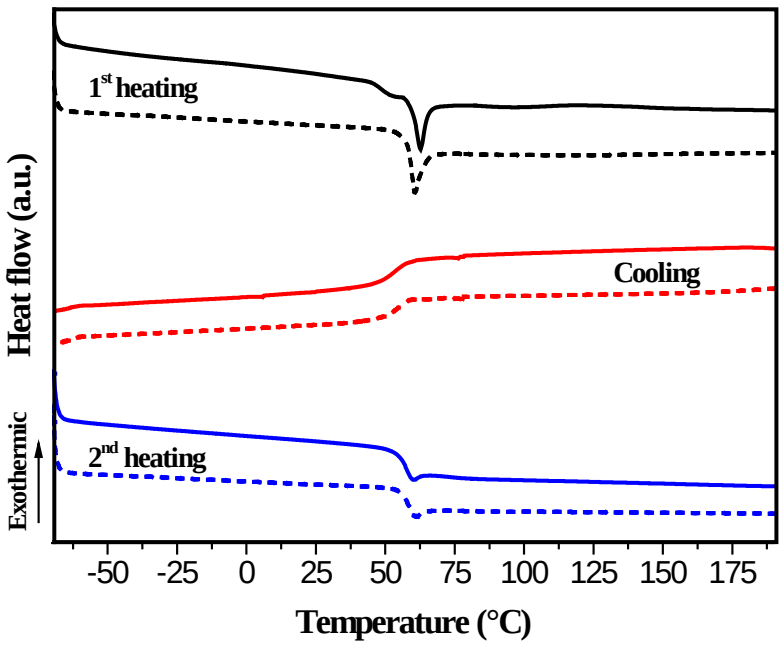

**Figure 10.** DSC thermograms derived from one cycle of heating-cooling-heating of PDLLA mat (solid lines) and pellets (dashed lines).

## 4. CONCLUSIONS

It was demonstrated that Forcespinning® is an alternative and straightforward technique to obtain PDLLA fibers in the sub-micron regime. The performed experiments showed that polymer concentration within the solution and selected angular speed have a strong influence on the morphology of materials derived from solutions of PDLLA in chloroform. Structures ranging from beads to homogeneous fibrous materials can be obtained. Furthermore, it was possible to establish the conditions under which sub-micron fibers are obtained; *ca* concentration of 10 wt.% in a range of angular speed of 8000 to 10000 rpm. At this concentration the production of homogeneous fibers was attributed to a suitable solution entanglement number (ca. 3.5), which was not significantly altered by the angular speed. The obtained fibrous materials have suitable morphological features ($\overline{D_f}$ ≤ 1 µm, Ø > 90%, homogeneous fibers with a uniform surface roughness) for applications in tissue regeneration.

## 5. ACKNOWLEDGEMENTS

The authors thank National Council for Science and Technology (CONACYT, México) for providing Victoria Padilla Gainza with a PhD grant as well as financial support for her research stay at the University of Texas Rio Grande Valley (UTRGV, US). The authors also thank Enrique Jimenez (CIQA, México) for the facilities related to viscosity measurements, Anabel Ochoa and Maria Guadalupe Méndez (CIQA, México) for their technical support in the evaluation of the thermal properties (TGA and DSC), and Hilario Cortez (UTRGV, US) and Jesús Angel Cepeda Garza (CIQA, México) for their technical assistance in electron microscopy characterization. The authors also acknowledge support received from National Science Foundation under PREM grant DMR 1523577.

## 6. REFERENCES

1. Bhattarai, D. P.; Aguilar, L. E.; Park, C. H.; Kim, C. S. *Membranes.* **2018***, 8,* 1-24.

2. Jun, I.; Han, H. S.; Edwards, J. R.; Jeon, H. *Int. J. Mol. Sci.* **2018**,*19***,** 1-14.

3. Ellison, C. J.; Phatak, A., Giles, D. W., Macosko, C. W.; Bates, F. S. *Polymer.* **2007**, *48*, 3306–3316.

4. Smith, L. a.; Ma, P. X. *Colloids Surfaces B Biointerfaces*. **2004**, *39*, 125–131.

5. Liang, H. W.; Guan, Q.F.; Chen, L.F.; Zhu, Z.; Zhang, W. J.; Yu, S.H. *Angew. Chem. Int. Ed.* **2012**, *51*, 5101–5105.

6. Zhang, X.; Lu, Y. *Polym. Rev.* **2014**, *54,* 677–701.

7. Huang, Z. M.; Zhang, Y. Z.; Kotaki, M.; Ramakrishna, S. *Compos. Sci. Technol.* **2003**, *63,* 2223–2253.

8. Sebe, I., Szabó, B., Nagy, Z. K., Szabó, D., Zsidai, L., Kocsis, B. & Zelkó, R. *Int. J. Pharm.* **2013***, 458***,**99–103.

9. Padron, S., Fuentes, A., Caruntu, D. & Lozano, K. *J. Appl. Phys.* **2013**, *113***,** 1-9

10. Padron, S.; Patlan, R.; Gutierrez, J.; Santos, N.; Eubanks, T.; Lozano, K. *J. Appl. Polym. Sci.* **2012**,*125,* 3610–3616.

11. Badrossamay, M. R.; McIlwee, H. A.; Goss, J. a.; Parker, K. K. *Nano Lett.* **2010**, *10*, 2257–2261

12. Ren, L.; Pandit, V.; Elkin, J.; Denman, T.; Cooper, J. A.; Kotha, S. P. *Nanoscale*. **2013**, *5*, 2337–2345.

13. Shenoy, S. L.; Bates, W. D.; Frisch, H. L.; Wnek, G. E. *Polymer.* **2005**, *46,* 3372–3384.

14. Lu, Y.; Li, Y.; Zhang, S. *Eur. Polym. J.* **2013**, *49*, 3834–3845.

15. Cai, Y.; Gevelber, M. *J. Mater Sci*. **2013**, *48*, 7812–7826.

16. Casper, C. L.; Stephens, J. S.; Tassi, N. G.; Chase, D. B.; Rabolt, J. F. *Macromolecules.* **2004***, 37*,573–578.

17. Vazquez, B.; Vasquez, H.; Lozano, K. *Polym. Engr. Sci.* **2012**, *52*, 2260–2265.

18. Gundogdu, N. a. S.; Akgul, Y.; Kilic, A. *Aerosol Sci. Technol.* **2018**, *52*, 515–523.

19. Rodríguez-Tobías, H.; Morales, G.; Ledezma, A.; Romero, J.; Grande, D. *J. Mater. Sci.* **2014**, *49,* 8373–8385.

20. Ramier, J.; Bouderlique, T.; Stoilova, O.; Manolova, N.;Rashkov, I.; Langlois, V.; Renard, E.; Albanese, P.; Grande.; D. *Mater. Sci. Eng. C*. **2014**, *38,* 161–169.

21. Graessley, W. W. *Adv. in Polym. Sci*. **1974**, *16*, 1–179.

22. Wang, C.; Chien, H.; Yan, K.; Hung, C.; Hung, K. *Polymer.* ***2*009**, *50,* 6100–6110.

23. Mead-hunter, R.; King, A. J. C.; Mullins, B. J. *Langmuir*. **2012**, *28*, 6731–6735.

24. Driessen, T.; Jeurissen, R.; Wijshoff, H.; Toschi, F.; Lohse, D. *Physics of Fluids.* **2013**, *25*, 062109.

25. Hong, X.; Edirisinghe, M.; Mahalingam, S. *Mater. Sci. Eng.* **2016,** *69***,** 1373–1382.

26. Adam, M.; Delsanti, M. *J. Phys.* **1982,** *43,* 549–557.

27. Megelski, S.; Stephens, J. S.; Bruce Chase, D.; Rabolt, J. F. *Macromolecules*. **2002**, *35***,** 8456–8466.

28. Lakshmi, N.; Jackie, N.; Aravind, D.; Suzhu, Y.; Manan, M. A. *RSC Adv.* **2014**, *4,* 44082–44088.

29. Wang, Z.; Zhao, C.; Pan, Z. *J. Colloid Interface Sci.* **2015**, *441,* 121–129.

30. Lin, J.; Ding, B.; Jianyong, Y.; Hsieh, Y. *ACS Appl. Mater. Interfaces*. **2010**, *2,* 521–528.

31. Roeder, R. K.; Converse, G. L.; Kane, R. J.; Yue, W. *Biol. Mater. Scienece.* **2008,** *60,* 38–45.

32. Pang, X.; Zhuang, X.; Tang, Z.; Chen, X. *Biotechnol. J.* **2010**, *5,* 1125–1136.

33. Salas, C.; Thompson, Z.; Brattarai, N. in *Electrospun nanofibers*; Afshari, M., Eds.; Woodhead Publishing, **2017**; Vol. 186, Charter 15, pp 317–398.

34. Oliveira, J. E.; Mattoso, L. H.; Orts, W. J.; Medeiros, E. S. *Advances in Materials Science and Engineering.* **2013**. 1-14.

35. Li, L. ; Huang, W.; Wang, B.; Wei, W.; Gu, Q.; Chen, P. *Polym.* **2015**, *68***,** 183–194.

36. Puchalski, M.; Kwolek, S.; Szparaga, G.; Chrzanowski, M.; Krucińska, I. *Polymers.* **2017**, *9,* 1-13.

**Graphical Abstract Figure**

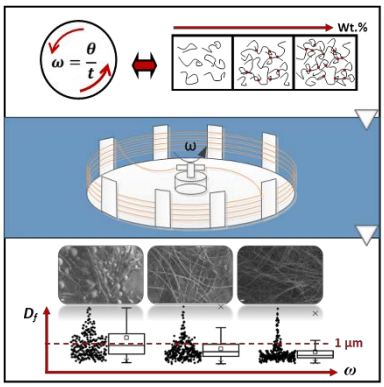

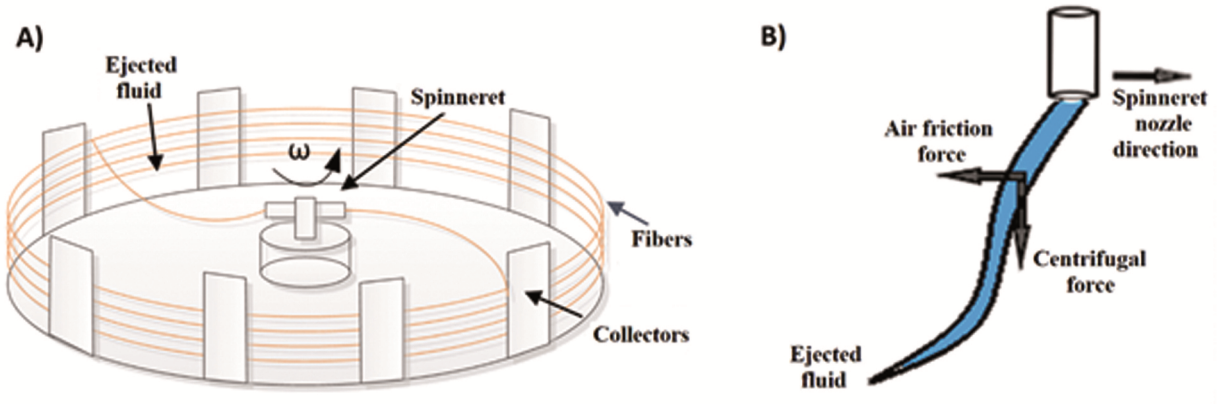


APP_47643_Figure 1.jpg

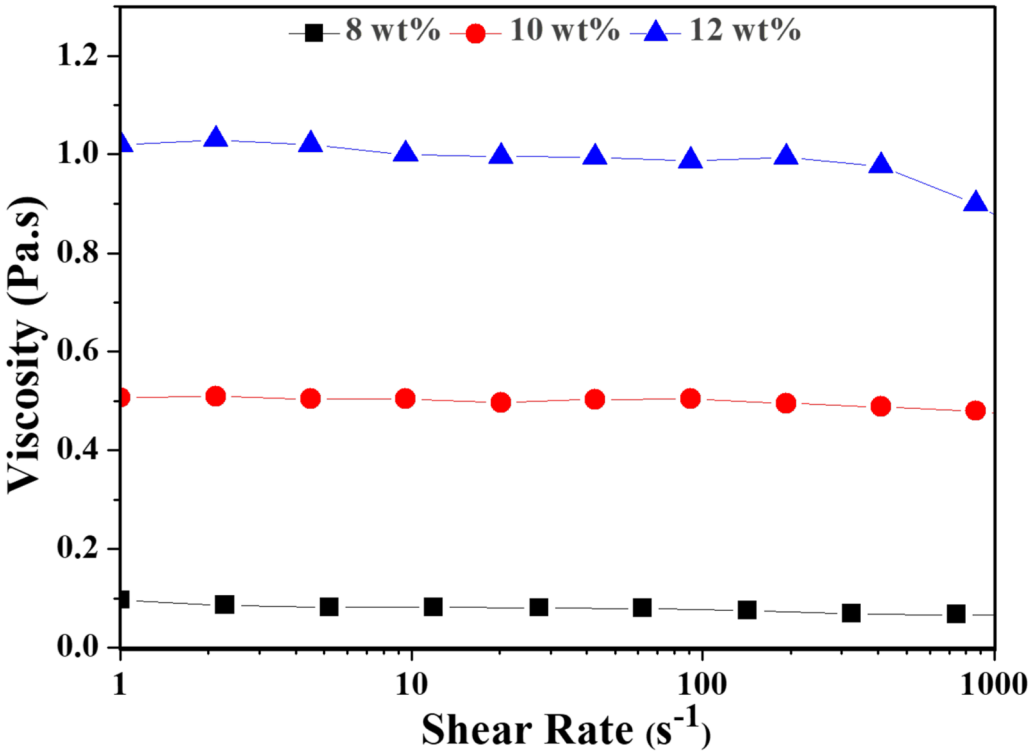


APP_47643_Figure 2.tif

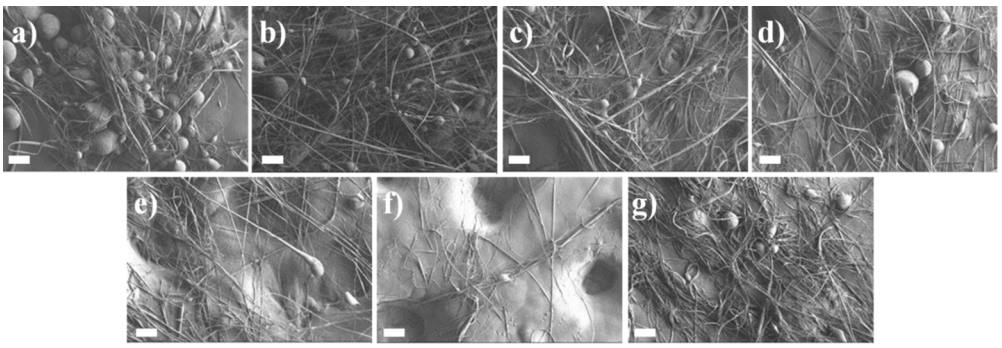


APP_47643_Figure 3.tif

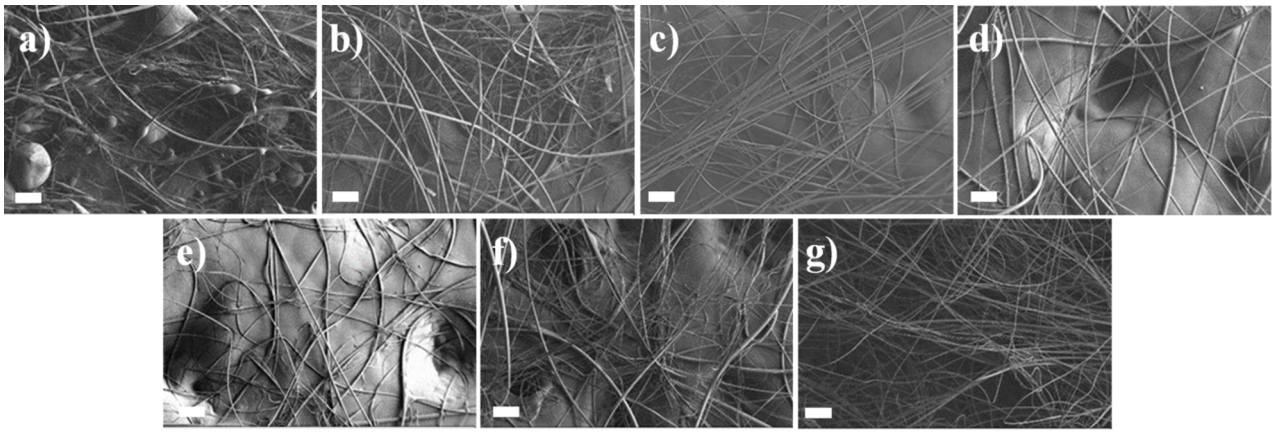


APP_47643_Figure 4.tif

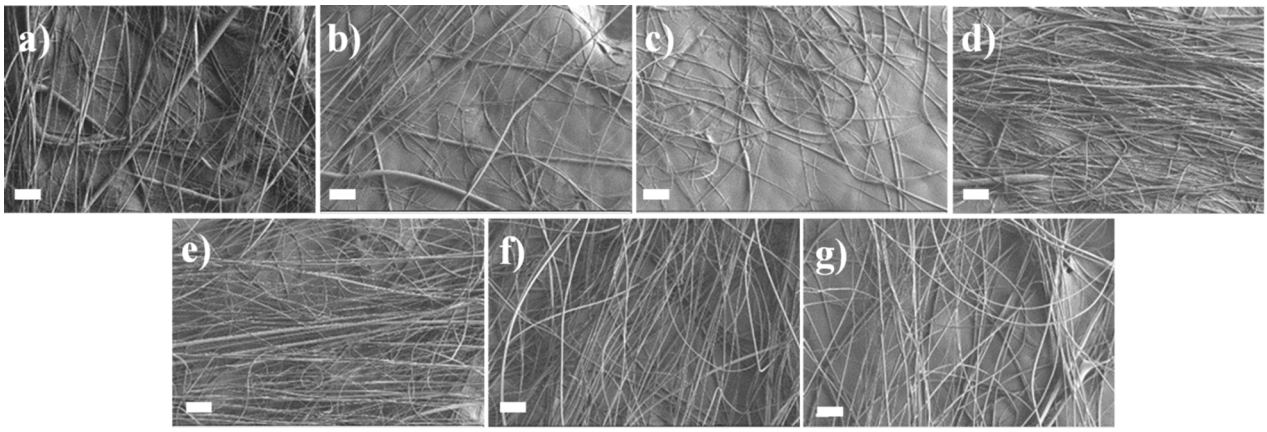


APP_47643_Figure 5.tif

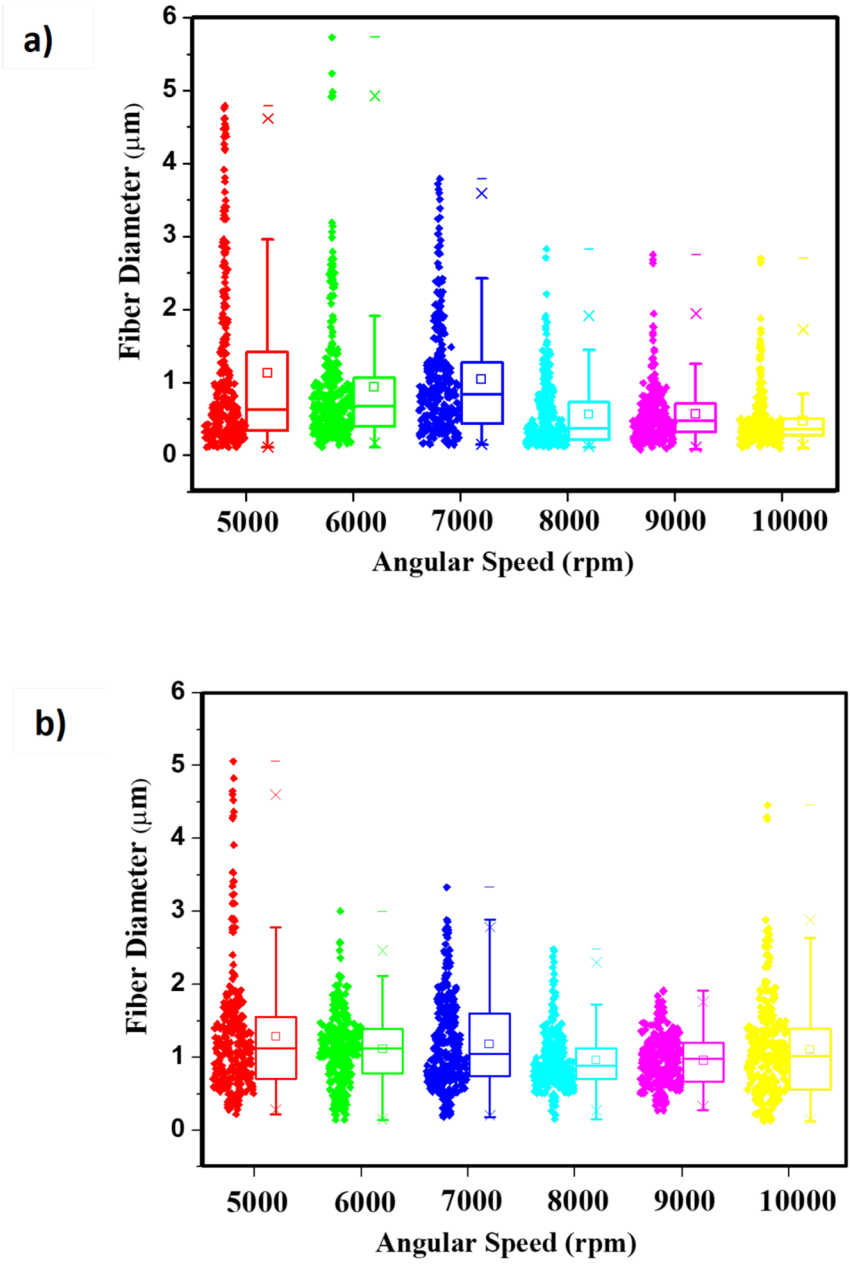


APP_47643_Figure 6.tif

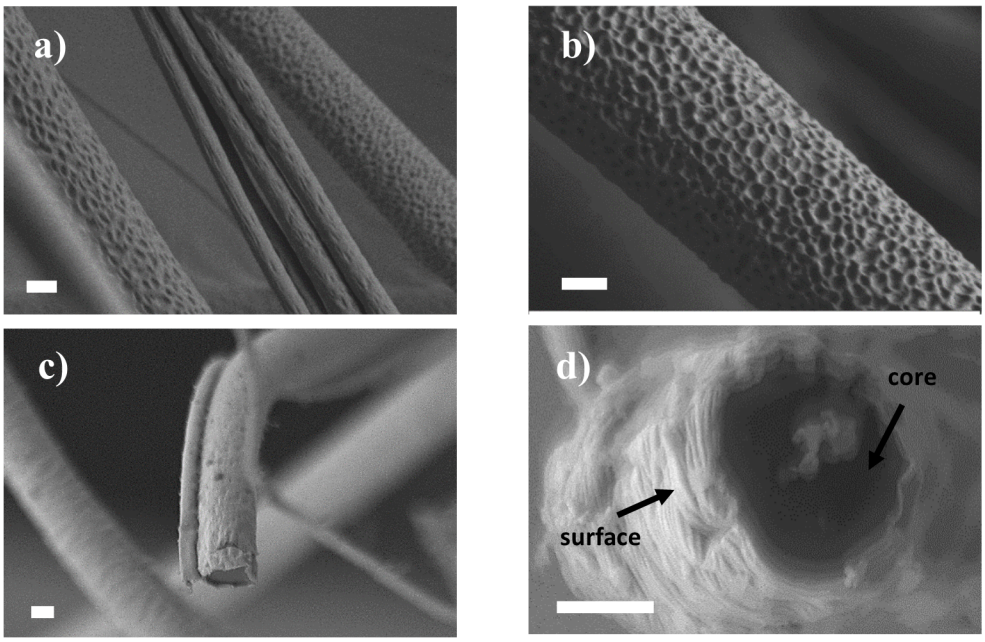


APP_47643_Figure 7.tif

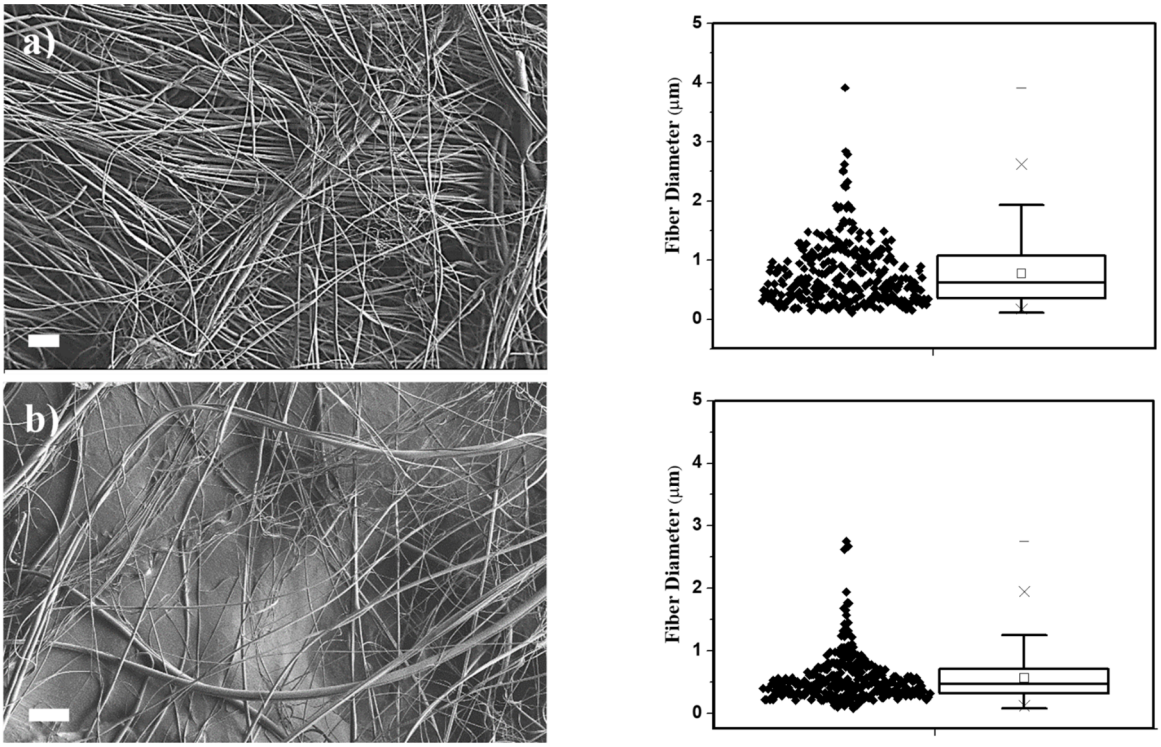


APP_47643_Figure 8.tif

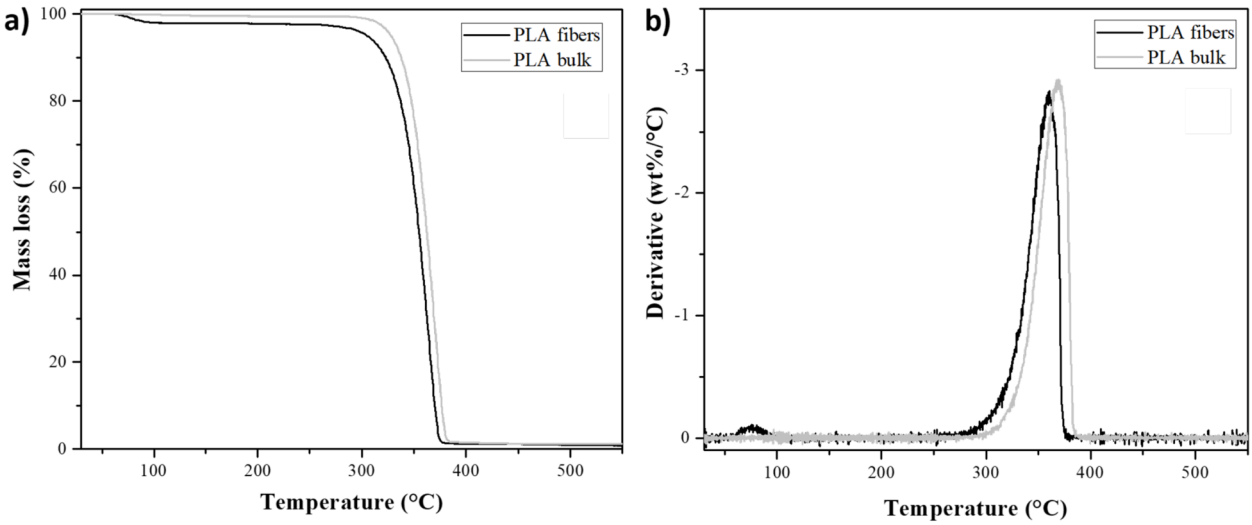


APP_47643_Figure 9.tif

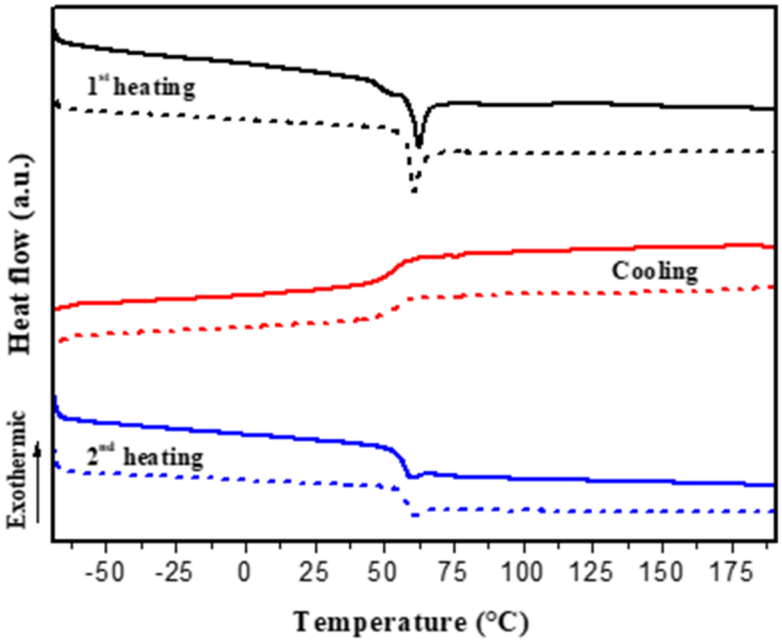


APP_47643_Figure 10.tif

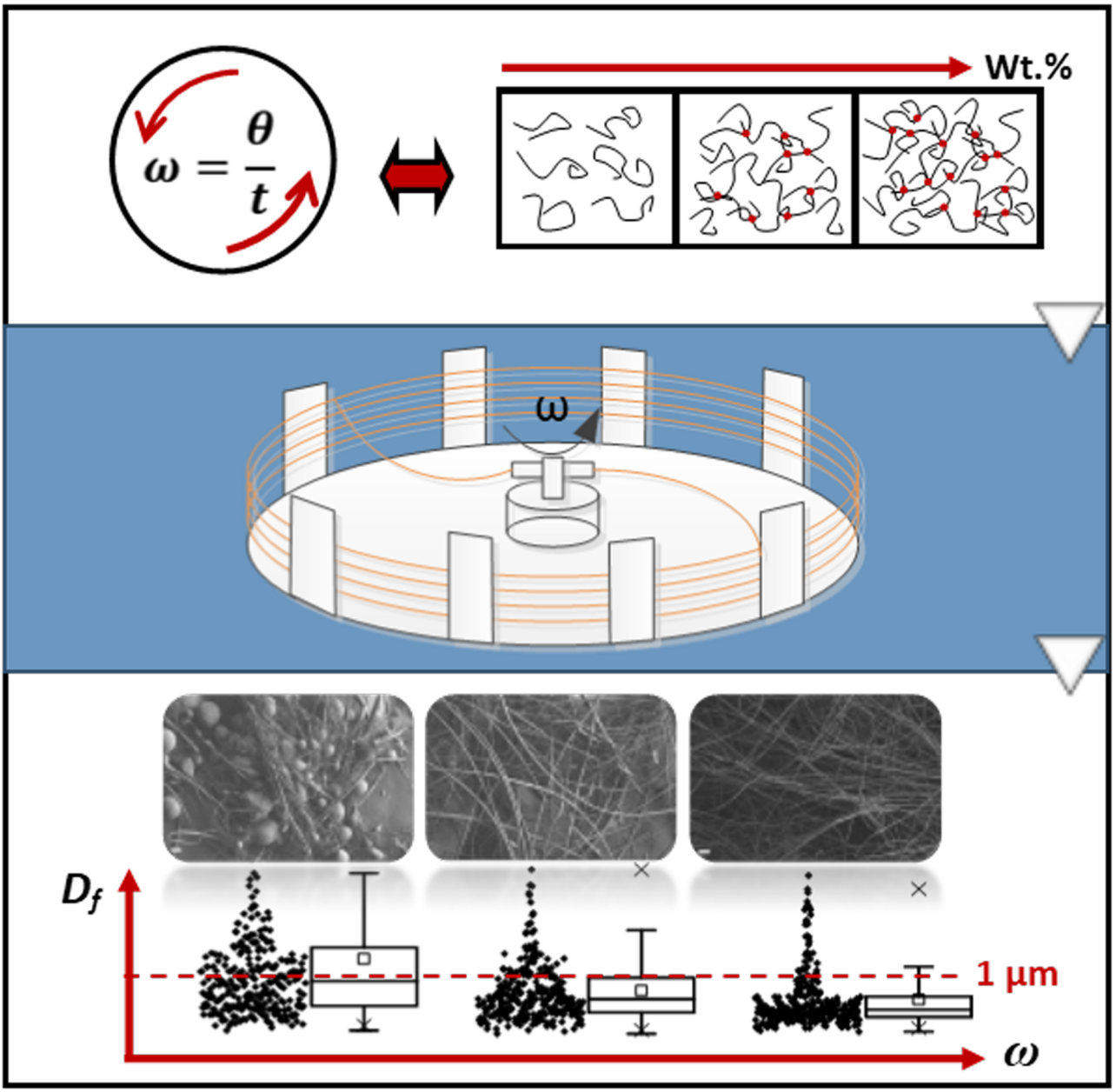


APP_47643_Graphical Abstract.tif